

Modeling the Structure of the Sea Anemone, Stomphia Coccinea and the Sea Star, Dermasterias Imbricata Using Implicit Surfaces

Xikun Liang
xkliang@cpsc.ucalgary.ca

Mai Ali Nur
mnur@cpsc.ucalgary.ca

Brian Wyvill
blob@cpsc.ucalgary.ca

Department of Computer Science
University of Calgary
2500 University Dr. NW, Calgary, Canada

Abstract

The *BlobTree* provides a hierarchical data structure for the definition of complex models built from implicit surfaces, CSG Boolean operations and space warping functions. The implicit model within the system is defined as a hierarchical composition of multiple objects. In this paper, we describe an application of the *BlobTree* to create visually accurate models of two invertebrates, the sea anemone, Stomphia Coccinea, and the sea star, Dermasterias Imbricata. The sea star was created using a variety of parameters that could be modified to create different variations of the Dermasterias Imbricata species. We use the phyllotactic method to obtain an accurate and visually pleasing arrangement of the sea anemone's tentacles. Using a hierarchical construction of the model, we can refine the model locally and deform it globally while maintaining the integrity of surface details. Taking advantage of the hierarchical representation of the object, we can easily adjust the model by simply changing some parameters of the surface or by performing global deformations on the anemone or local refinements on the tentacles.

Key words: Implicit surfaces, hierarchical surfaces, modeling, local refinement, global deformation, marine creatures, spiral phyllotaxis, collision detection.

1 Introduction

An implicit surface S is characterized as a collection of points in space with a potential $f(x, y, z)$ equal to some threshold value denoted by T .

$$S = \{M(x, y, z) \in \mathcal{R}^3, f(x, y, z) = T\}$$

Modeling with Implicit surfaces guarantees a continuous smoothly blended surface which is relatively easy to deform and intuitive to specify. Since invertebrates are animals lacking backbones and many of them have small, soft, flabby bodies, implicit objects are ideal to model these spongy structures. We have chosen to model the structure and behavior of two such creatures, the sea

star and sea anemone. Not only do these creatures have stunningly beautiful variations in structure but they also exhibit interesting behaviors.

One of the best studied and most dramatic escape responses of marine invertebrate is the detachment and swimming behavior of Stomphia (S. Coccinea and S. Didemnum) in response to certain species of starfish such as Dermasterias Imbricata [3]. The escape response of the Stomphia Coccinea from Dermasterias Imbricata has been of great interest to scientists ever since it was first described in 1955 by Yentsch and Pierce [30] and has resulted in a variety of studies on different aspects of the interaction: behavioral [19] [21], neurophysiological (the discipline involving the study of the makeup and function of the nervous system) [20] morphological (a branch of biology that deals with the form and structure of animals and plants) [17], ecological [16] and chemical. The main aim behind this paper is to create realistic models of Stomphia Coccinea and Dermasterias Imbricata that can be used to study the structure and behavior of these marine creatures. In this paper we focus on creating these structures procedurally. As a result, adjustment of various parameters produced different sea stars and changed the structure of the sea anemone.

The tentacles of the anemone are correctly positioned by using the phyllotactic method. The hierarchical representation of the model allows the structure to be easily animated and locally and globally deformed. The paper is organized as follows. In section 2, we summarize previous work in this area. Section 3 provides a detailed description of the models to be developed. We explain the general behavior of the sea anemone and sea star in section 4. Section 5 describes the modeling implementation details. Section 6 presents our conclusions and future work.

2 Related work

Previous relevant work will be discussed in this section. The *BlobTree* and the hierarchical implicit surface re-

finement technique, used to build the models, and the collision-based spiral phyllotaxis approach used to position the anemone's tentacles are outlined.

2.1 The *BlobTree*

The *BlobTree* [28] provides a hierarchical data structure for the definition of complex models built from implicit surfaces, CSG Boolean operations and field warping functions. The implicit model within the system is defined as the hierarchical composition of multiple objects (Figure 1). The surface of an implicit object can also use attributes such as 2D textures. The *BlobTree* has been extended to incorporate textures as described in [25].

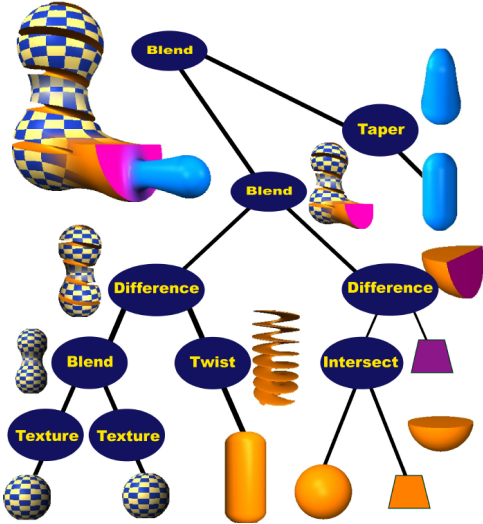


Figure 1: Example of a model built up from a *BlobTree* [28]

2.2 Hierarchical Implicit Surface Refinement

Since the implicit surface models built from the *BlobTree* are basically static models. Once defined, the *BlobTree*'s structure can't be easily changed. To further extend the use of the *BlobTree*, a hierarchical implicit surface refinement technique has been proposed in [15]. This method consists of hierarchical representation and construction of implicit objects.

- **Hierarchical Representation of Implicit Surfaces**

For a given implicit object, we create a hierarchy of implicit surfaces representing the object. In the hierarchy, each surface is a node in the tree, either an internal node at the coarser level or a leaf node at a finer level. Each hierarchy contains a local surface and a set of sub-hierarchies. The surface defined by the *BlobTree* is a leaf node relative to the higher level hierarchy. Each sub-hierarchy is an internal

node in the overall structure and it represents local surface detail. Surface details related to a specific surface being refined are within the same hierarchical level. With this representation, implicit objects at each level consists of the local surface S_{global}^i and all the surfaces of its sub-hierarchies $\sum S_{sub-surface}^i$ at level i:

$$S_{surface}^i = S_{global}^i OP_{refinement} \sum S_{sub-surface}^i.$$

where $OP_{refinement}$ represents the operation of the hierarchy.

This hierarchical structure of implicit surfaces is illustrated by Figure 2.

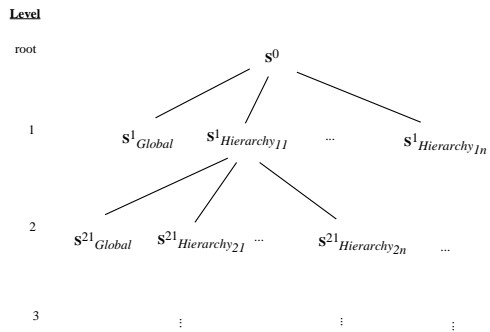


Figure 2: Hierarchy of the implicit object

According to the refinement operations, four kinds of hierarchies are designed:

- Blending
- Controlled Blending
- Precise Contact Modeling
- CSG

They represent four different kinds of operations combining the global surface with its details. Blending uses super-elliptic blending method described in [1]. Controlled blending is implemented by the method proposed in [9]. Precise contact modeling combines the local surface and surface details using the approach described in [6]. CSG operations perform intersection, difference, or union between the local surface and the refined surface.

- **Surface Construction**

We start with an initial implicit surface and create a root hierarchy with the surface. A sequence of sub-hierarchies can be built by recursively refining the selected surfaces. At each level, a set of refined

surfaces S^i are introduced to define local surface details.

The final implicit object is obtained by combining all the leaf surfaces according to the different kinds of hierarchical properties. The lower level are processed first. Then the surface constructed at that layer is combined with its higher level surfaces using blending, controlled blending, precise contact modeling, or CSG operations. The process continues until all the terminal surfaces are included. Due to the hierarchical construction of the refining surface, local details can be maintained according to the constraints for each refinement.

The advantages of this method are the ability to apply hierarchical local refinement and global deformation to the models. Local refinement allows the user to introduce more detailed surfaces at any given level. Global deformation changes the overall shape of the surface while maintaining the integrity of surface details.

2.3 The Collision-based Model of Spiral Phyllotaxis

This section gives a general overview of spiral phyllotaxis and its application to generate collision-based models. Phyllotaxis is the regular arrangement of organs such as flowers or leaves often seen in many plants. It is characterized by spirals or parastichies, composed of sequences of adjacent organs forming the structure. The number of parastichies running in opposite directions are usually two consecutive Fibonacci numbers [5]. The divergence angles, taken from the center of the structure, measured between consecutive formed organs is close to the Fibonacci angle of $360^\circ \tau^{-2} = 137.5^\circ$ where $\tau = (1 + \sqrt{5})/2$. The quality of the pattern generated depends on this angle [18]. This mathematical formula has lead to both descriptive and explanatory models of phyllotaxis [12]. Descriptive models are like those proposed by Vogel [26] and Van Iterson [4] [11], they attempt to capture the geometry of phyllotactic patterns. Explanatory models, focus on the dynamic process controlling the formulation of phyllotactic patterns in nature. There are a large number of competing theories for explanatory models and unfortunately, no universally accepted model has emerged [12]. In this paper we use the collision-based model of phyllotaxis described in [5] which combines the descriptive and explanatory components with slight modifications to satisfy the properties needed to create the tentacles on the sea anemone.

The collision-based model of phyllotaxis proposed in [5] is used to distribute primordia on the surface of the receptacle. Primordia are a group of cells that can be initially identified as a future body part. As described in [5],

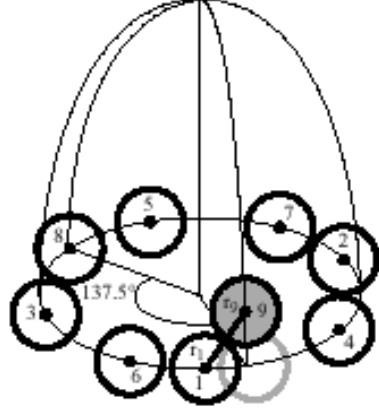


Figure 3: The collision-based model of phyllotaxis. Primordia are distributed on the receptacle using a fixed divergence angle of 137.5° and are displaced along the generating curves to become tangent to their closest neighbors. Courtesy images of [5]

the receptacle is viewed as a surface of revolution, generated by a curve rotated around a vertical axis. Spheres which represent primordia are added to the structure sequentially with a divergence angle of 137.5° . A horizontal ring at the base of the receptacle is formed by this initial group of primordia. When a primordium just added collides with an existing one, the addition of primordia, to this ring stops. The colliding primordium are moved along the generating curve, tangent to its closest neighbor. The next group of primordia are placed similarly, on generating curves tangent to their closest neighbors, determined by the divergence angle as shown in Figure 3. The addition of primordia continues until there is no more room to add another one. Since the anemones we are modeling have a flower-like tentacle arrangement, we use this phyllotactic method to arrange tentacles of varying sizes on arbitrary surfaces of revolution. It can therefore be used to create a wide variety of sea anemones.

3 Properties of *Coccinea Stomphia* and *Dermasterias Imbricata*

This section gives a general description of the marine creatures to be created, followed by a more detailed description of the specific species to be modeled.

3.1 *Stomphia Coccinea*

Anemones or the flower animal as they are often called, have a single body cavity that serves as a stomach, intestine and circulatory system. They fasten themselves to something firm with their bases and have one body opening (the mouth), through which everything passes

in or out. The mouth is surrounded by finger-like tentacles, studded with nematocysts (stinging cells). Nematocysts are active in capturing food and transferring it to the mouth for defense.

The five main components of *Stomphia Coccinea* obtained from, the textural descriptions found in [24] [22] and observations of pictures in [10] are explained below:

1. **The column** which is cylindrical and not divided into regions. It is never as wide as the base or disk. The outer membrane is generally thin and often transparent and always smooth. It can have a series of strange forms. In contraction, the column is low, firm and dense. In extension the body is soft and the skin becomes smooth and translucent when sufficiently extended. The color of the column ranges from solid orange to pale white. Many are pale orange with irregular orange or red areas scattered on the column.
2. **The base** which is adherent, slightly irregular and much wider than the column is used to attach the anemone to the substrate.
3. **The upper disk** is circular and transparent with orange patches scattered on it. There is a large central area which is free of tentacles, where there is a slit for the mouth. The surface of the disk is often irregular.
4. **The tentacles** which surround the mouth may be up to 1.5 cm long, conical, and fully covered when retracted; there can be 64 but there are usually 72, although individuals with as many as 86 can be found. They are generally arranged in four or five cycles with those of the inner cycles being slightly longer than those of the outer ones. The six tentacles of the first or inner cycle are usually held pointing inward over the disk, whereas those of the outer two or three cycles bend down over the margin. The color of the tentacles are white or transparent with two orange rings encircling them and a small white spot at the base of each.

The *Stomphia Coccinea* is up to 3 or 4 cm tall with the column being usually less than 3 cm in diameter. The disk of a specimen this size would be about 3 cm wide and the base about 5 cm.

3.2 Dermasterias Imbricata

This section describes the general features of the sea star and features specific to *Dermasterias Imbricata*. Sea stars vary in shape, size and color. They can be from less than 1/2 of an inch in diameter to more than 3 feet across. Their shapes vary from regular stars with five or more

arms to pentagonal and almost circular sea stars [2]. The most common colors found in sea stars are orange, yellow, pink, or red but gray, green, blue and purple colors can also be found. The arms of sea stars are actually part of its body rather than appendages. If one of these animals is turned upside down to expose its mouth surface, each arm is seen to have a lengthwise groove filled with moving tube-feet. Within each arm the star has one or two branches of its reproductive organs and often extensions from the digestive tract as well. The starfish that will be modeled is the *Dermasterias Imbricata* or the Leather star. It has slightly webbed rays usually 5 that are up to 12 cm in length. Its skin is smooth and slippery and feels like wet leather. *Dermasterias Imbricata*'s body comes in a variety of colors. However it is usually mottled with reddish brown to orange blotches outlined with grey. It possesses a large, high disk at the center of the body and the tips of its arm are frequently upturned. A rather unusual property of it, is the fact that it often has a strong odor of garlic.

4 The General Behavior of the Anemone and Starfish

This section describes the interaction between the *Coccinea Stomphia* and *Dermetrias Imbricata*. Although we have not yet animated the models, it is interesting to observe the variations in the model's structure over time as illustrated in Figure 4. A number of parameters associated with our models will enable us, in the future, to create a realistic animation. For example, the anemone has various lengths, widths for each component and spacing parameters for the tentacles, and random bending angles. For the starfish these parameters include the length of the legs and their angles and the dimensions used. By adjusting these parameters our structures could easily be adapted to different interaction situations between the anemone and starfish.

The general pattern of the swimming behavior in *Stomphia Coccinea* described was illustrated in detail both through a diagram, shown in Figure 4 and from a textural description taken from [3]. The interaction between the *Dermasterias Imbricata* and *Stomphia Coccinea* consists of a number of phases:

1. *The stimulus phase* occurs when the surface of the starfish *Dermasterias Imbricata* comes in brief contact with the anemone's tentacles.
2. *During the initial response phase*, the anemone's tentacles adhere to the starfish on contact. After several seconds the tentacles contract, followed at once by contraction of the column.

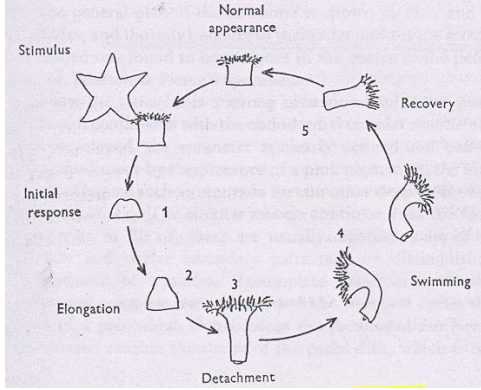


Figure 4: The swimming behavior in Stomphia of the anemones

3. *The elongation phase* occurs when the column elongates. The tentacles and disk then reappear and expand to their fullest extent.
4. *The detachment phase* occurs when the pedal disk of the anemone becomes detached. This phase is variable, as an anemone may show swimming movements without detaching from the substratum.
5. *The swimming phase* consists of a series of abrupt bending movements of the column, which may cause the animal to ‘swim’.
6. *The recovery phase* is an inactive period during which the anemone resumes its normal shape. The surface of the pedal disk then becomes adhesive, and so it re-attaches to the substratum and the ordinary permanently attached position is regained.

Although the swimming response of Stomphia is variable, nearly all anemones which respond to *Dermasterias* display the initial response, expansion usually followed by detachment or the swimming movement [3]. If the swimming movement occurs then recovery is the last phase. Detachment may be regarded as a side effect and doesn't always take place.

5 Implementation details

In this section the procedures used to model the sea anemone and sea star will be described.

5.1 Modeling the Anemone

The anemone is modeled using hierarchical implicit surface refinement approach. The main body is first created as the root hierarchy. Then a CSG hierarchy is introduced to model the mouth which takes the difference of the main body from a line primitive. The tentacles are added as the

third layer. All the tentacles are created in two consecutive layers. The First layer models the main branch of the tentacle and the second models the tip of the tentacles. They are positioned following the phyllotactic pattern.

When modeling the tentacles we have chosen to assume that they surround the mouth in 4 cycles $6, 12, 18, 36 = 72$ or $6, 10, 16, 32 = 64$ (with 6 being the innermost cycle), taken from [24]. These formulas are subject to minor irregularities, affecting the outer tentacles on the whole more than the inner ones. The following sections describe details for building the model.

The Main Body

The main body consists of the base, the column and the disk (components 2,1,3 in section 3.1). A cylinder was used for the body and a torus was used for the base and upper disk. All three objects were blended together as shown in Figure 5 (left).

The mouth of the anemone is modeled with the CSG difference operation. A line primitive is subtracted from the main body to create a mouth in the center of the upper disk (Figure 5(right)). The tentacles will be positioned around this mouth.

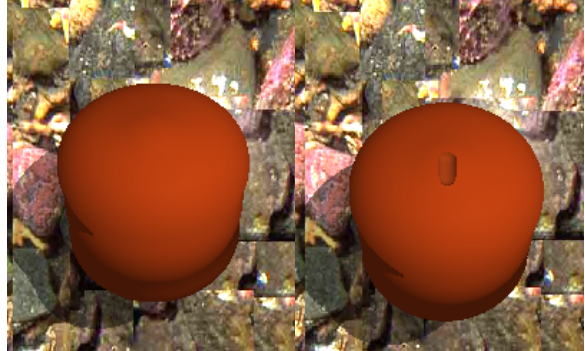


Figure 5: The main body is a blend of two tori and a cylinder and the mouth was created by applying a CSG difference between the main body and a line primitive

The Tentacles

The tentacles are created using a tapered line primitive. They are initially placed on a plane and then shifted to the implicit surface of the main body moving from the outer cycle to inner cycles. Based on the collision-based model of the spiral phyllotaxis as described in section 2.3, a new algorithm is created to accurately place the tentacles on the implicit surface. The general procedure is outlined below:

- **Formalization:** In order to calculate the positions of the tentacles, we first assume that the tentacles are placed on the plane of the anemone’s upper disk as



Figure 6: Tentacles are positioned in a circle using the modified Phyllotactic approach

shown in Figure 6. The initial position is described by the parametric equation:

$$\begin{cases} x = r \cos(\theta), \\ y = r \sin(\theta), \\ z = \text{body height} \end{cases}$$

where r is the radius of the circle under consideration and θ is the orientation of the tentacles separated with 137.5^0 . The tentacles are placed sequentially with an angle of 137.5^0 following the pattern illustrated in Figure 3.

- **Formulation of layered tentacle pattern:** With this simple algorithm, the new tentacle may collide with a tentacle at the same layer. In this case, instead of moving the tentacle directly to the next inner layer, we search the current layer for any possible position. If such a place cannot be found, it is then moved to the next inner layer. This recursive formulation of the tentacle pattern can be described as follows:

$$\begin{cases} \theta_0 = 0, \\ r = D, \text{ the top disk radius}, \\ \\ \theta_{n+1} = \theta_n + 137.5^0 = (n + 1) * 137.5^0 \\ r_{n+1} = \begin{cases} r_n, & \text{not collided}, \\ r_n - \epsilon, & \text{collided}, \end{cases} \end{cases}$$

where r is the radius of the current layer. When a collision occurs, a new radius r_{n+1} is obtained by subtracting the diameter of the current tentacle from r_n . If collision still exists, we simply adjust the radius by a predefined step size ϵ .

With this algorithm, the angle θ at which the new tentacle will be placed is at $(n+1) \cdot 137.5^0$. However,

The angle varies when collision occurs. Addition of tentacles to a single layer isn't terminated until each layer follows the pattern 6,12,18,36, described at the beginning of this section.



Figure 7: Tentacles are moved tangent to the anemone's top surface

- **Surface searching:** Furthermore, the pattern generated so far only provides tentacle positions at the plane of the anemone's upper disk (Figure 6). Since the body is a smoothly blending surface, some of the tentacles may appear inside or outside of the top surface. Therefore the tentacles are placed tangent to the surface. This is achieved by moving all the tentacles to the surface. We first check if the tentacle's position given by the previous formulas is inside or outside of the surface. We then choose an opposite point along the normal and find the point on the surface, i.e. $f(x, y, z) = \text{iso_value}$. The assumptions made were that the surface used for calculating the phyllotactic tentacle position is a section of the upper disk of the anemone and that the radius of the intersection is within the bounding box. The algorithm is outlined below:

1. Calculate the possible tentacle position $P(x, y, z)$ according to the modified phyllotactic model,
2. Calculate the bounding box of the body,
3. Find the normal of $P(x, y, z)$ on the surface, i.e.

$$N(x, y, z) = (f_x, f_y, f_z)$$

where f is the field function of the implicit surface and f_x , f_y , and f_z are the partial derivatives of the field function at P .

4. Find a point Q inside the surface if $f(P) < \text{iso_value}$ or a point Q outside the surface if $f(P) > \text{iso_value}$. This can be done simply by searching along the surface normal with a

given step size. In this case, an inside or outside point is guaranteed to be found as long as the step size is less than the radius of the body.

5. Search the exact corresponding surface point of P along the line between the inside and outside points P and Q . A binary search method was implemented to find the surface position.

Figure 7 shows the tentacle pattern after this process. The tentacles are also oriented along the surface normals.

Anemone Deformations

This section describes the deformation of the tentacles and the main body. Anemone tentacles exhibits various shapes and deformations. They have slightly different sizes at each layer and all tend to bend in certain directions as described in 3.1. This is achieved by placing the tentacles according to the normals and the phyllotactic angles.

The outer tentacles bend over the margins, the innermost ones bend inwards, while the rest bend randomly. All tentacles are oriented based on several noise functions. These functions were applied to the bending angle, bending center, bending range, and orientations as shown Figure 8. Other functions such as the 4D noise functions described in [29] could be used to provide better control over the tentacles' appearance.

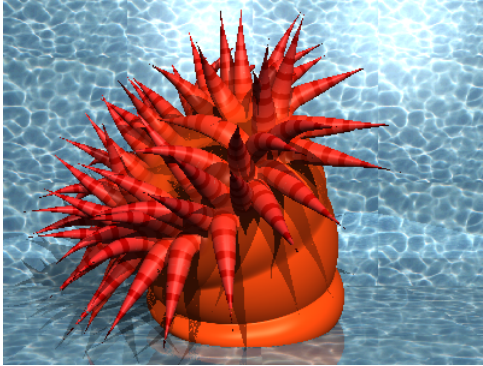


Figure 8: Body deformation with automatic maintenance of tentacle integrity

An anemone's body is deformed when it is stimulated by another object, such as a starfish. The tentacles and body experience various stages of deformation as described in section 4. Since the anemone is constructed hierarchically as stated at the beginning of section 5.1, global deformation can easily be applied to any part of the object. To model the bending characteristics of the anemone, global deformation is applied to the main

body. Then all the tentacles are automatically adjusted to maintain the integrity of the structure. Figure 8 shows a anemone body bent 270 degrees.

Final anemone models

Two anemones were created using our proposed method. Textures were applied to the anemone's main body and tentacles. Figure 9 shows an anemone model with the 64 tentacles and figure 10 illustrates the typical 72 tentacles. Both of these anemones have been rotated by 45 degrees. As can be seen, the tentacles follow the phyllotactic pattern. The outer layer tentacles are bent sharply against the body and have an outward orientation. The second and third layer tentacles are slightly bent and randomly oriented. The inner layer tentacles bend inwards. Overall, the tentacles arrangement shows the beauty of the phyllotactic pattern and the randomness applied creates more lively looking sea anemones.

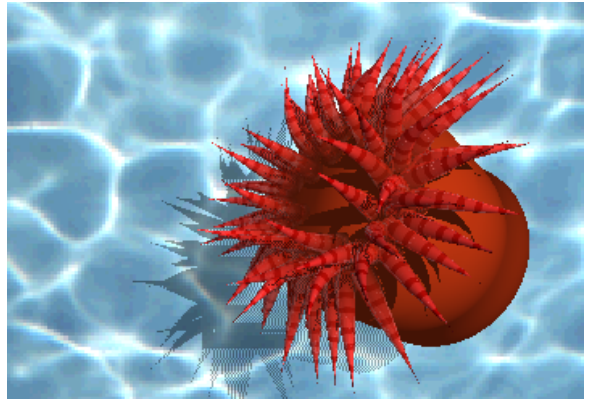


Figure 9: An anemone with 64 tentacles around the upper disk



Figure 10: An anemone with 72 tentacles around the upper disk

5.2 Modeling the Starfish

The starfish was modeled as described below:-

1. Five cones were created for the arms.
2. The star's arms were rotated and translated to the correct positions. They were rotated to lie in the $X - Z$ plane and were translated to lie in a circle. The initial position is described by the parametric equation:

$$\begin{cases} x = r \cos(\theta), \\ y = r \sin(\theta), \\ z = \text{body height} \end{cases}$$

Where r is the radius of starfish surface. The angles used were measured from a picture of the starfish.

3. A texture was applied to the cones (Figure 11 (left)).



Figure 11: Starfish legs are created using cone primitives and the correct texture was applied (left). A bump surface was created using point primitives (right)

4. Small bumps were created along the cone primitives. The top surface of the starfish we choose had a rather unusual texture that required the use of point primitives to achieve the surface texture. Unlike some starfish, our example had a irregular surface. To create the texture, a grid like pattern of points was created on each cone (Figure 11 (right)). The spheres were moved to the surface of the cone using the surface searching method described in section 5.1. A Random offset was subtracted from the position of the sphere so that some spheres would be hidden in the surface. Therefore the final texture would consist of some irregularities to achieve more realistic model. The spheres were blended with each other and control blended with the surface. Controlled blending of the spheres with the surface allowed the shape and texture to be clearly observed as shown in Figure 12.

5. Random colors were applied to all point primitives selected from 6 brown colors that were found on the starfish (Figure 12).



Figure 12: The final bump texture was created by moving the point primitives tangent to the surface with a random noise function applied

A similar approach was applied to create another leather star, that had a very different texture. The point primitives were moved tangent to the surface but this time only a few were added to the center. They were added using random angles and random radius values. The final model of this sea star's legs were slightly bent as in Figure 13.



Figure 13: Another Leather Starfish with a different surface appearance

6 Conclusions and Future work

In this paper we have presented a method to model two invertebrates, the sea anemone, *Stomphia Coccinea*, and

the sea star, Dermasterias Imbricata as an application of the *BlobTree*. The model combines implicit surfaces, CSG, controlled blending, 2D texture mapping and the collision-based model of phyllotaxis. The results show implicit surfaces being capable of modeling complex sea creatures using a procedural approach. We are currently working on generating more realistic images using rendering techniques such as Photon maps [13, 14] to correctly reproduce the effect of transparency and translucency, observed in some of these creatures. We are looking towards creating a realistic simulation of the behavior of these marine creatures, using a physically based approach. We have found that the *BlobTree* provides an excellent structure on which to base such models. Using the techniques of Cani-Gascuel and Desbrun, [8], we intend to simulate the interactions between these objects and their environment. We are investigating the extension of the *BlobTree* to incorporate these features to provide better tools for implicit modeling.

7 References

- [1] J. Bloomenthal, C. Bajaj, J. Blinn, M. P. Cani-Gascuel, A. Rockwood, B. Wyvill, and G. Wyvill. Introduction to Implicit Surfaces. Morgan Kaufmann Publishers Inc., California, 1997.
- [2] R. Buchsbaum and L. J. Milne. Living Invertebrates of the World. Hamish Hamilton LTD, London, 1960.
- [3] J. K. Elliot, D. M. Ross, C. Pathirana, S. Miao, R. J. Anderson, P. Singer, Kokke W. C. M. C. and Ayer W. A. Induction of Swimming in Stomphia (Anthozoa: Actiniaria) by Imbricate, A Metabolite of the Asteroid Dermasterias Imbricata. In *Biological Bulletin*, 176:73-74, April 1989.
- [4] R. O. Erickson. The Geometry of Phyllotaxis. In *J. E. Dale and F. L. Milthrop, editors, The Growth and Functioning of leaves*, pages 53-88. University Press, Cambridge, 1983.
- [5] D. R. Fowler, P. Prusinkiewicz, J. Battjes. A Collision-based Model for Spiral Phyllotaxis. In *Computer Graphics*, 26(2), July 1992.
- [6] M. P. Gascuel. An Implicit Formulation for Precise Contact Modeling Between Flexible Solids. In *SIGGRAPH'93, Computer Graphics Proceedings*, pages 313-320, 1993.
- [7] M. P. Cani-Gascuel. Layered Models with Implicit Surfaces. In *Graphics Interface'98*, pages 201-208, Vancouver, Canada, June 1998.
- [8] M. P. Cani-Gascuel and M. Desbrun. Animation of Deformable Models Using Implicit Surfaces. In *IEEE Transactions on Visualization and Computer Graphics*, 3(1):pages 39-50, 1997.
- [9] A. Guy and B. Wyvill. Controlled Blending for Implicit Surfaces. *Implicit Surfaces'95*, April 1995.
- [10] R. M. Harbo. whelks To Whales. Coastal Marine Life Of The Pacific Northwest. Harbour publishing, BC, Canada, 1949.
- [11] G. Van Iterson. Mathematische und Mikroskopische-Anatomische Studien Über Blattstellungen. Gustav Fischer, Jena, 1907.
- [12] R. V. Jean. Mathematical Modeling in Phyllotaxis: The State of the Art. In *Mathematical Biosciences*, 64:pages 1-27, 1983.
- [13] H. W. Jensen, J. Legakis and J. Dorsey. Rendering of Wet Materials. In *Rendering Techniques '99*. Eds. D. Lischinski and G. W. Larson. Springer-Verlag, pages 273-282, 1999
- [14] H. W. Jensen. Global Illumination Using Photon Maps, In *Rendering Techniques'96*. Eds. X. Pueyo and P. Schrder. Springer-Verlag, pages 21-30, 1996.
- [15] X. Liang. Hierarchical Modeling of the *BlobTree*. Research Report No.99/561/11, University of Calgary, Department of Computer Science, 1999.
- [16] K. P. Mauzey, C. Birkeland and P. K. Dayton. Feeding Behavior of Asteroids and Escape Responses of Their Prey in the Puget Sound Region. In *Ecology*, 49(4), 1968.
- [17] D. J. Petuya. An Anatomical Study of the Nervous System and Some Associated Tissues of the Anemone Stomphia Coccinea. PHD thesis, University of Alberta, Canada, 1976.
- [18] P. Prusinkiewicz and A. Lindermayer. The Algorithmic Beauty of Plants. Springer-Verlag, New York, 1990. With J. Hanan, F. D. Fracchia, D. R. Fowler, M. J. M. de Boer, and L. Mercer.
- [19] E. A. Robson. Some Observations on the Swimming Behavior of the Anemone Stomphia Coccinea. In *Journal of Experimental Biology*, 38:pages 343-363, 1961.
- [20] E. A. Robson. The Swimming Response and its Pacemaker System in the Anemone Stomphia Coccinea. In *Journal of Experimental biology*, 38:pages 685-694, 1961.
- [21] D. M. Ross. A Third Species of Swimming Actinostoid (Anthozoa: Actiniaria) on the Pacific Coast of North America. In *Canadian Journal of Zoology*, 57:pages 943-945, 1979.

- [22] A. E. Siebert. A Description of the Sea Anemone *Stomphia Didemon* sp. nov. and its Development. In *Pacific Science*, 27(4):pages 363-376, 1973.
- [23] J. M. Shick. A Functional Biology of Sea Anemones. Chapman and Hall, London, 1991.
- [24] T. A. Stephenson. The British Sea Anemones. Ar-lard and Son, Limited, London, Great Britain, 1934.
- [25] M. Tigges and B. Wyvill. Texture Mapping the BlobTree. In *Implicit Surfaces '98*, June 1998, pages.123-130.
- [26] H. Vogel. A Better Way to Construct the Sunflower Head. In *Mathematical Biosciences*, 100:pages 161-199, 1990.
- [27] J. A. Ward. An Investigation on the Swimming Reaction of the Anemone *Stomphia Coccinea*, II. Histological Location of a Reacting Substance in the Asteroid *Dermasterias Imbricata*. In *Journal of Experimental Zoology*, 158:pages 365-370, 1965.
- [28] B. Wyvill, A. Guy, and E. Galin. Extending the CSG Tree Warping, Blending and Boolean Operations in an Implicit Surface Modeling System. In *Implicit Surfaces '98*, pages 113-121, June 1998.
- [29] G. Wyvill and K. Novins. Filtered Noise and The Foruth Dimension. In <http://atlas.otago.ac.nz:800/geoff/graphics/Noise.html>, 1998.
- [30] C. S. Yentsch and D. C. Pierce. Swimming Anemone from Puget Sound, 122:pages 1231-1233, 1955
- [31] R. Zonenschein, J. Gomes, L. Velho, and L.H. Figueiredo. Texturing Implicit Surfaces with Particle Systems. In *Technical Sketch in Visual Proceedings SIGGRAPH 1997*, page 172, August 1997.